Agricultural Water Management 213 (2019) 1096–1108

Contents lists available at ScienceDirect

Agricultural Water Management

journal homepage: www.elsevier.com/locate/agwat

Spatial and temporal characteristics of reference evapotranspiration and its climatic driving factors over China from 1979–2015

Zongzhi Wang[a,*], Ailing Ye[a,b], Lihui Wang[b], Kelin Liu[a], Liang Cheng[a]

[a] State Key Laboratory of Hydrology-Water Resources and Hydraulic Engineering, Nanjing Hydraulic Research Institute, Nanjing 210029, China
[b] College of Civil Engineering, Fuzhou University, Fuzhou 350002, China

ARTICLE INFO

Keywords:
Reference evapotranspiration
Climate change
Aridity index
Sensitivity analysis
Spatiotemporal characteristics

ABSTRACT

The reference evapotranspiration (ET_0) has decreased over most of China under climate change over the past few decades, especially before the 1990s, which significantly affects the agricultural water requirements. In this study, the recent tendency of ET_0 over China was determined and the issues of what causes this tendency and how this tendency would affect agricultural water demand were discussed. First, we evaluate ET_0 (consisting of the aerodynamic term ET_{0_a} and the radiative term ET_{0_r}) using the Penman-Monteith method based on the grid-based China Meteorological Forcing Dataset (CMFD) from 1979 to 2015. Second, we analyze the trends of ET_0 and five climatic variables using the Mann-Kendall test and the Sen's slope estimator. Finally, we assess the impacts of meteorological factors on ET_0 by calculating dimensionless sensitivity coefficients and contribution rates. Based on the ET_0 results and precipitation data, we also evaluate the aridity index (AI) over China to explore the impacts of the tendency of ET_0. The result of the trend analysis of ET_0 reveals that there is a significantly increasing trend after the 1990s over China, and this trend could be attributed to the increasing air temperature based on the results of the contribution rates, where ET_0 is most sensitive to the specific humidity. The AI result reveals a decreasing trend over the study period, which indicates that the irrigation water supply could be appropriately reduced on the premise of proper and scientific utilization of water due to the more significantly increasing availability of water even though the water demand for evapotranspiration increased.

1. Introduction

Evapotranspiration plays an essential role in the hydrological cycle and agriculture water management and has observably changed under climate changes and intensified human activities (Hoffman, 2010; Seo et al., 2012). The actual evapotranspiration consisting of evaporation from the land surface and transpiration from crops is difficult to directly measure on a wide scale owing to specific devices, difficulties of accurate measurements and relatively high costs (Liu et al., 2013). Thus, evapotranspiration is commonly estimated from weather data, so-called reference evapotranspiration (ET_0), which is a key indicator of actual evapotranspiration (Zhang et al., 2015). ET_0 represents the evapotranspiration ability of a hypothetical reference crop with a specific height, surface resistance and albedo and without water stress, which is important to assess agriculture water demand. To estimate ET_0, the Penman-Monteith method considering a radiative term and aerodynamic term is a fairly reliable method requiring air temperature, radiation, wind speed and humidity data and is used as a standard method in many studies (Fan et al., 2016; Wang et al., 2017).

Over the past several decades, remarkable changes in temperature (Stocker et al., 2014), radiation (Tang et al., 2011), wind speed (Young et al., 2011) and humidity (Dai, 2006) have caused variations in ET_0. Generally, there was a decreasing trend in ET_0 over China and the most significant decline occurred in southern China, which was difficult to reconcile with the significant increase in temperature over the past few decades (Thomas, 2000; Liu et al., 2011; Fan and Thomas, 2018). The variation of ET_0 is a consequence of variations in all meteorological factors, and understanding the impacts of climate change on ET_0 is helpful to predict actual evapotranspiration and agriculture water demand.

In recent years, extensive research has aimed at exploring the spatial and temporal characteristics of ET_0 and the effects of climate on ET_0. There are several kinds of commonly used methods: (1) statistical methods, (2) sensitivity analyses, and (3) contribution rate analyses. Sensitivity (McCuen, 1974) and contribution rate (Liu et al., 2009; Yin et al., 2010) analyses are more quantitative than statistical methods such as regression and significance testing. Zongxing et al. (2014) explored the impacts of meteorological factors on ET_0 in southwestern

* Corresponding author.
E-mail address: wangzz77@163.com (Z. Wang).

https://doi.org/10.1016/j.agwat.2018.12.006
Received 18 July 2018; Received in revised form 9 November 2018; Accepted 3 December 2018
Available online 08 January 2019
0378-3774/ © 2018 Elsevier B.V. All rights reserved.

China using multiple regression analysis. McVicar et al. (2007) developed an 'interpolate-then-calculate' method to consider the topographic influence on meteorological data based on a spline model with a linear sub-model. McVicar et al. (2012) focused on the near-surface wind speed trend on a globe scale by reviewing and synthesizing many studies to demonstrate the contributions of aerodynamic components to ET_0 change. For China as a whole, the decreasing trend of ET_0 before the 1990s that ran counter to the increase in temperature was mainly attributed to the remarkable declines of near-surface wind speed (Feng et al., 2014) and radiation (Thomas, 2000) in many studies, while the climatic drivers influencing ET_0 are regionally different. Employing a nondimensional relative sensitivity coefficient, Gong et al. (2006) studied the sensitivities of meteorological factors to the variation of ET_0 in the Yangtze River Basin, and the result revealed that ET_0 was most sensitive to relative humidity. Chen et al. (2006) quantified the variation of driving climatic factors to ET_0 in the Jinghe River catchment, northern China and found that the ET_0 was most sensitive to relative humidity, while the contribution of wind speed and sunshine hours was the greatest owing to their relatively large variations. In accordance with these aforementioned studies, it can be seen that the variation of a meteorological factor that changes ET_0 the most may not be the factor that ET_0 is the most sensitive to.

However, there are few synthetic studies on the impacts of the driving factors on ET_0 both nationally and regionally in China using multiple methods, and the mechanisms responsible for changing ET_0 remain uncertain. China is one of the most populous countries in the world, having a large food pressure, and the variation of ET_0 caused by climate change has a profound impact on food security and welfare in China. Meanwhile, with the advancement of meteorological data, the quality of basic data can affect the accuracy of results, and the data used in most existing studies are based on meteorological stations. Thus, the recent analysis of characteristics and drivers of ET_0 over China using higher-density data is meaningful. To fill this gap, this paper investigates three issues: the variations of ET_0 and meteorological factors, the contributions of climate work on ET_0 and how the variations of ET_0 will influence agricultural water management.

Based on grid data of climate and elevation over China, the spatial distribution and trends of temperature (maximum and minimum), radiation, wind speed, humidity and ET_0 are estimated both nationally and regionally. The commonly used Penman-Monteith method is used to calculate ET_0 consisting of the radiative term (ET_{0_r}) and aerodynamics term (ET_{0_a}). To explore the mechanisms of how climatic factors influenced ET_0, we analyze the trend of ET_0 using the Mann-Kendall test and the Sen's slope estimator, which are also used to estimate the trends of meteorological variables. We investigate the driving factors on different spatial scales by calculating the sensitivity coefficients and contribution rates of meteorological variables. The main intention of this paper is to offer some information for agriculture water management and help understand the mechanisms of ET_0 change caused by climate change through exploring the trend of ET_0, its drivers and trend of AI over China in recent years.

2. Methodology

2.1. Study area and data

The remarkable regional diversity of natural condition in China results in the spatial characteristics of meteorological factors over China. Wetness and temperature are the critical factors influencing regional farming system and the features of them in China show an uneven distribution, where the north is drier and colder than the south. To explore the influences of meteorological factors on ET_0 over China and offer suggestions of agricultural water management, the study area is divided into seven regions in accordance with the properties of geography, land use type, climate and farming system, including northwest China (NW), northeast China (NE), northern China (NC), central China (CC), eastern China (EC), southern China (SC) and southwest China (SW) (Fig. 1). The detailed properties of regions are shown in Table 1. The eastern (NE, EC, CC and SC) is greatly influenced by the monsoon climate and the rainfall there concentrates mainly in summer. The southwest (SW) belonging to the plateau climate features in low temperature, strong radiation, less rainfall and low atmospheric pressure. The northwest (NW and NC) situates the inland with dry climate, scarce precipitation and intensive evaporation. The climatic data used to calculate ET_0 are from the China Meteorological Forcing Dataset (CMFD) developed by Data Assimilation and Modeling Center for Tibetan Multi-spheres, Institute of Tibetan Plateau Research, Chinese Academy of Sciences. The dataset is produced through merging a variety of data sources including China Meteorological Administration station data for 1979–2015, GEWEX-SRB (Global Energy and Water cycle Experiment - Surface Radiation Budget) downward shortwave radiation for 1983.07–2007.12, and GLDAS (Global Land Data Assimilation System) downward shortwave radiation data for 1979.01–1983.06 and 2008.01-2010.12. The applicability and reliability of the CMFD dataset has been verified in other researches (Xue et al., 2013). Chen et al. (2011) used this dataset to simulate the surface temperature in arid and semi-arid regions of China and the simulated result was satisfactory. The spatial resolution of the climatic data is 0.1 °, and the temporal resolution is 1 day. Daily data are available for the maximum and minimum temperature ($Tmax$ and $Tmin$, K), specific humidity (q, kg·kg^{-1}), atmospheric pressure (P, Pa), wind speed measured at 2 m above the surface (u_2, m·s^{-1}) and downward shortwave radiation (R_s, W·m^{-2}). The spatial resolution of the elevation data is 0.1 ° (700 × 400) by resampling elevation data with a higher resolution using ArcGIS (ESRI, Redlands, California).

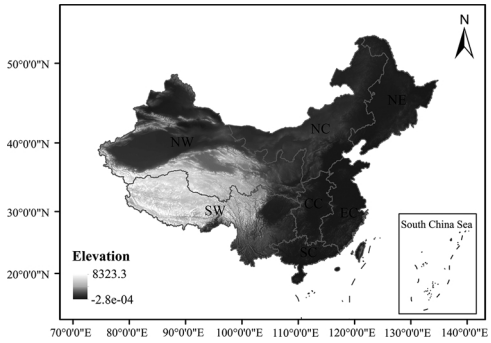

Fig. 1. The distribution of seven partitions of the study area. The study area is divided into seven subregions based on geography, land use type, climate and farming system. In addition to the climate types mentioned above, it is worth noting that the Tibetan Plateau is located mostly in SW and partially in NW.

2.2. The FAO56 penman-monteith method

The Penman-Monteith method was selected to calculate daily ET_0 in this paper, which was recommended by FAO (Food and Agriculture Organization) in 1998 (Allen et al., 1998). Based on theories of energy balance and mass transfer, the Penman-Monteith equation has a relatively solid theoretical basis and is applicable to humid and arid regions (Mcmahon et al., 2012; Odhiambo et al., 2005; Xu et al., 2010). The equations to calculate daily ET_0 and its two components are shown as:

$$ET_0 = ET_{0_r} + ET_{0_a} = \left(\frac{0.408\Delta(R_n - G)}{\Delta + \gamma(1 + 0.34u_2)}\right) + \left(\frac{\gamma\frac{900}{T+273}u_2(e_s - e_a)}{\Delta + \gamma(1 + 0.34u_2)}\right) \quad (1)$$

where R_n is net radiation at the crop surface [MJ m^{-2} day^{-1}], G is soil heat flux density [MJ m^{-2} day^{-1}] (in daily ET_0, G is negligible), T is mean daily temperature measured at 2 m [°C] (derived by the average of $Tmax$ and $Tmin$), u_2 is the near-surface wind speed measured at 2 m

Table 1
Main properties of seven regions of China.

Region	Geography	Land use type	Farming system	Climate
Northwest China (NW)	Basin, mountains	Desert, grassland	One harvest per year	Temperate continental
Northeast China (NE)	Plain	Forest, dry land	One harvest per year	Temperate monsoon
Northern China (NC)	Plateau	Desert, grassland, dry land	Three harvests in two years	Temperate continental and monsoon
Central China (CC)	Plain, hill	Dry land, paddy field	Two harvests per year	Subtropical monsoon
Eastern China (EC)	Plain	Paddy field, forest	Two harvests per year	Subtropical monsoon
Southern China (SC)	Hill	Paddy field, forest	Two to three harvests per year	Tropical and subtropical monsoon
Southwest China (SW)	Plateau, basin	Grass land, forest, desert	One to two harvest per year	Alpine, subtropical monsoon

[m s^{-1}], e_s is the saturation vapor pressure [kPa], e_a is actual vapor pressure [kPa], Δ is the slope vapor pressure curve [kPa°C^{-1}], and γ is the psychrometric constant [kPa °C^{-1}].

The net radiation is estimated based on R_s data from the CMFD through the equations in FAO paper 56 (Allen et al., 1998). Due to the availability of relative humidity data, the actual vapor pressure is calculated using the following equation (Verburg and Hecky, 2003) instead of the method given in FAO paper 56:

$$e_a = \frac{Pq}{0.378q + 0.622} \tag{2}$$

where q is the specific humidity [kg kg^{-1}], and P is atmospheric pressure [kPa].

2.3. Mann-Kendall test and Sen's slope estimator

The Mann-Kendall test (M-K test) is a nonparametric trend test that is applicable for analyzing non-normally distributed data, and the sample data are not necessary compliant with the specific distribution (Hirsch and Slack, 1984). By the M-K test, the trend of ET_0 can be quantified, and the comparison of trends among regions is more intuitionistic. In the null hypothesis of the M-K test, when the length of the data set is over 8, the test statistic is approximately compliant with a normal distribution with a mean value equal to zero. The procedures to calculate test statistics, the variance of test statistic, and the standardized test statistic are as follows:

$$S = \sum_{i=1}^{n-1} \sum_{j=i+1}^{n} \operatorname{sgn}(x_j - x_i) \tag{3}$$

$$VAR(S) = \frac{n(n-1)(2n+5) - \sum_{i=1}^{n} t_i(t_i-1)(2t_i+5)}{18} \tag{4}$$

$$Z = \begin{cases} \frac{S-1}{\sqrt{VAR(S)}} & S>0 \\ 0 & S=0 \\ \frac{S+1}{\sqrt{VAR(S)}} & S<0 \end{cases} \tag{5}$$

where S is the test statistic, VAR is the variance of S, Z is the standardized test statistic, n is the total number of sample data, x_j and x_i are the yearly mean values of year i and j, and t is the extent at any given time. If $|Z| > Z_{1-\alpha/2}$, the null hypothesis is rejected with a given confidence level α; namely, there is a significant trend in the time series data $\{X\}$. When α is equal to 0.05 and 0.01, $Z_{1-\alpha}$ is equal to 1.960 and 2.576, respectively. If $Z > 0$, there is an increasing trend of S, which means the sample data $\{X\}$ exhibit the same trend. Contrarily, if $Z < 0$, $\{X\}$ exhibits a decreasing trend.

The slope of trend of data is evaluated by the non-parametric Sen's slope estimator developed by Sen in 1968 (Sen,1968). It is calculated as:

$$\beta = Median\left(\frac{x_j - x_i}{j - i}\right), \forall\, j > i \tag{6}$$

where x_j and x_i are data values at times j and i. The median of the ascending sequence of values $\{(x_j\text{-}x_i)/(j\text{-}i)\}$ reflects the Sen's slope estimator and then the confidence interval of the slope can be calculated as follows:

$$\begin{aligned} &C_\alpha = Z_{1-\alpha/2}\sqrt{VAR(S)} \\ &M_{1,2} = (N \pm C_\alpha)/2 \\ &P\{X_{(M_1)} < \beta < X_{(M_2+1)}|\beta\} = 1-\alpha \end{aligned} \tag{7}$$

where $Z_{1-\alpha}$ and $VAR(S)$ are defined as mentioned previous. N is the length of the ascending series $\{(x_j\text{-}x_i)/(j\text{-}i)\}$ written as X, and $X_{(M1)}$ represents the M_1th values in series X. The Sen's slope estimator has been widely used in trend analysis of hydro-meteorological data (Gocic and Trajkovic, 2013; Partal and Kahya, 2006).

2.4. Sensitivity analysis and contribution rate

The simple partial derivative of a climatic variable is able to reveal how the meteorological factors influence the ET_0 intuitively, while owing to the magnitudes of different variables, the partial derivative is inadequate to evaluate the sensitivities of each variable. Thus, we used a sensitivity function (McCuen, 1974) with the property of magnitude invariance to analyze the sensitivity of meteorological factors to ET_0 quantitatively. The sensitivity coefficient has been widely used in estimating the sensitivity in evapotranspiration (Darshana, Pandey and Pandey, 2013; Liu et al., 2009) and other hydrology(Shen and Yapa, 1986) or meteorology (Luxmoore et al., 1981) research. The sensitivity coefficient is defined by:

$$S_{x_i} = \lim_{\Delta x_i \to 0}\left(\frac{\Delta ET_0/ET_0}{\Delta x_i/x_i}\right) = \frac{\partial ET_0}{\partial x_i}\cdot\frac{x_i}{ET_0} \tag{8}$$

where S_{xi} is the sensitivity coefficient of the meteorological variable x_i, calculated on daily data and the final result of sensitivity coefficient is the annual mean values of daily values. The larger the absolute value of S_{xi} is, the more likely ET_0 is affected by the variable. The correlation between ET_0 and each variable depends on the positive or negative value of the sensitivity coefficient. If $S_{xi} > 0$, ET_0 will increase as the variable increases; if $S_{xi} < 0$, ET_0 will decrease as the variable increases. A sensitivity coefficient of 0.1 for a meteorological variable is equivalent to a 1% increase in ET_0 when the variable increases 10%.

The sensitivity coefficient indicates the extent of a meteorological variable influencing ET_0, while it does not need to be equivalent to the change in ET_0 caused by each variable. Here, we multiplied a partial derivative of a variable by its multi-year change rate to calculate the

'contribution rate' (Liu et al., 2009). A positive contribution rate means that the variation of a climatic factor has a positive effect on the variation of ET_0 and vice versa. The contribution rate is calculated as follows:

$$\frac{dET_0}{dt} = \frac{\partial ET_0}{\partial T_{max}}\frac{dT_{max}}{dt} + \frac{\partial ET_0}{\partial T_{min}}\frac{dT_{min}}{dt} + \frac{\partial ET_0}{\partial R_s}\frac{dR_s}{dt} + \frac{\partial ET_0}{\partial u_2}\frac{du_2}{dt} + \frac{\partial ET_0}{\partial q}\frac{dq}{dt} + \delta \quad (9)$$

where δ is the error item, and $\frac{dx}{dt}$ is calculated using the least square method.

2.5. Aridity index

We also discuss the variation of the aridity index, an indicator of agricultural water demand, which is meaningful to water resource management. It is defined as the quotient of the difference between ET_0 and precipitation and ET_0:

$$AI = (ET_0 - P)/ET_0 \quad (10)$$

AI less than or equal to 0 means that precipitation satisfies the reference evapotranspiration demand, and *AI* close to 1 indicates that aridity is heavy and crops need additional water supply. An increasing *AI* reflects a drier climate and may mean an increase in irrigation water supply and a decrease in crop yield (Tabari and Aghajanloo, 2013).

3. Results

3.1. Spatiotemporal characteristics of meteorological factors

The trends and spatial distribution of the five meteorological factors from 1979 to 2015 over China are evaluated in this paper based on the CMFD, including temperature (*Tmax* and *Tmin*), downward shortwave radiation (R_s), wind speed (u_2), and specific humidity (q). The nationwide distributions of the statistics Z of five meteorological factors derived by the M-K test are presented in Fig. 2 and the regional Sen's slope results are shown in Table 2.

On a national scale, the trend of climatic variables can be described as two stages with a demarcation of 1996. The observed interannual variation of *Tmax* and *Tmin* over China showed a more intensive increase during 1996–2015 than 1979–1996, with overall trends of 0.703 ˚C and 0.185 ˚C per decade, respectively. u_2 decreased during the former period and exhibited slight increasing trends during the latter period, which was opposite to the variation of q that decreased after an initial increase. The overall trend of R_s is insignificant. On a regional scale, every region experienced the increasing *Tmax* and the Sen's slope estimator of *Tmax* shows that NW and SW experienced greater warming than the other regions. The increasing R_s distributed partially in NW, SW and NC, and the decreasing R_s mianly distributed in some areas of NC, NW and SW. Although a wide-range decline of u_2 was found over China, a slight increase nevertheless occurs in some areas of SW and NW. The mean annual q over China was featured by a significant increase. The variations of five meteorological factors in different seasons were also evaluated in this study. It is worth noting that there is an obvious valley value of ET_0 (see Fig. 2) that occurs in 2012 and similar valley values of *Tmax*, *Tmin* and u_2 can be observed. The regional interannual rate of variables in all seasons are seen in Fig.3. Western China, SW and NW have experienced similar increasing *Tmax* in all seasons, and the dominant increasing trends of *Tmax* in spring occur in SC, EC and CC. *Tmin* in SW and NW also showed an increasing trend during all seasons, while increases of *Tmin* in other regions were much smaller. Most parts of China were featured by significantly decreasing R_s in summer, the change rate of which was larger in the south than the north. The variation of R_s in spring revealed that the transitional zone of humidity (partial areas of SW, NC and NE) had increasing R_s while other humid regions and arid regions had decreasing R_s. A decreasing trend of u_2 occurred in most parts of China, except SC, and significant declines in u_2 in all seasons were found in NE, NC and EC. It is noted that a significant increase in q occurs in autumn over China, except NC, and the variation rate of q in summer varies spatially and decreases progressively from north to south.

3.2. Spatiotemporal characteristics of annual ET_0

ET_0 calculated by the Penman-Monteith method over China exhibits an increasing trend after the 1990s, with a decreasing trend before the 1990s. As the highest value was found in the northern Sinkiang and Gansu Province, annual ET_0 in NW was larger than the other regions, especially NE and SW. The regional variation of annual ET_0 is shown in Fig. 4, where different areas of China exhibit increasing trends that are similar to the general trend of China. However, only NE experienced a decrease in ET_0, and ET_0 in EC remained relatively unchanged during the study period. The strong annual increase in ET_0 in SW and NW was supported by the Mann-Kendall test result, as the test statistical values Z in the two regions were over 1.96 (Fig. 4i). The significantly decreasing ET_0 mainly distributed in some areas of NE and EC. Fig. 4 also shows that significant valley values of ET_0 in 2012 can be found in all regions especially in NC, NE and NW. The distribution of seasonal variation in ET_0 is also remarkable (Fig. 5). In spring, most of China experienced an increase in ET_0 except NE, with a decreasing trend of -6.89 mm per decade. In summer, coastal regions of China showed a decreasing trend in ET_0 while inland areas of China exhibited an opposite trend, with NW and SW showing a significant increasing ET_0. In western and southern China, the ET_0 of autumn and winter were larger than those in eastern and northern China.

3.3. Monthly variation of ET_0 and climate within a year

Two components of ET_0, ET_{0_r} and ET_{0_a}, exhibit similar patterns of variation within a year, in that they both increase to the crest value and then decrease (see Fig. 6). Different in the start time of decreasing, ET_{0_r} increases to the crest value in spring (May), while ET_{0_a} starts to decrease in summer (June). The predominant component of ET_0 also varies within a year, in that ET_{0_r} plays a more important role during late spring, summer and early autumn, while ET_{0_a} slightly exceeds ET_{0_r} in winter. Variations of these two components both showed an overall increasing trend during 1979–2015, while ET_{0_a} first decreased from 1979 to 1996 and then increased during 1996–2015, which was opposite to the variation of ET_{0_r}. Concentrating on the interannual trends of seasonal ET_{0_a} and ET_{0_r}, it can be derived that variations of these two components of spring and summer characterize the trend of annual ET_{0_a} and ET_{0_r}. Thus, the most significant variation of ET_0 in spring in different regions can be explained. On the other hand, the significant valley values of seasonal ET_{0_a} occurring in 2012 are in accordance with the valley values of annual ET_0 and ET_{0_a}, which demonstrates the predominance of variation of ET_{0_a} in the variation of ET_0.

3.4. Sensitivity analysis of ET_0 to meteorological factors

3.4.1. Spatial distribution of sensitivity coefficients

As observed from Fig. 7, the sensitivity coefficient of *Tmax* (*STmax*) decreases progressively from the southeast to northwest over China, with the largest value found in EC and the smallest value found in NE. The spatial distribution of the sensitivity coefficient of *Tmin* (*STmin*) showed a pattern that is similar to *STmax*, and there was a discernable transition zone of *STmin* from the southeast to northwest. The sensitivity coefficient of R_s (SR_s) over China was positive. Different from the distribution of *STmax* and *STmin*, SR_s decreased progressively from south to north, with the largest value found in SC and the smallest value found in NW. Opposite to SR_s, the sensitivity coefficient of u_2 (Su_2) decreased from north to south over China, with the largest value found in NW and NE and the smallest value found in SW. The sensitivity

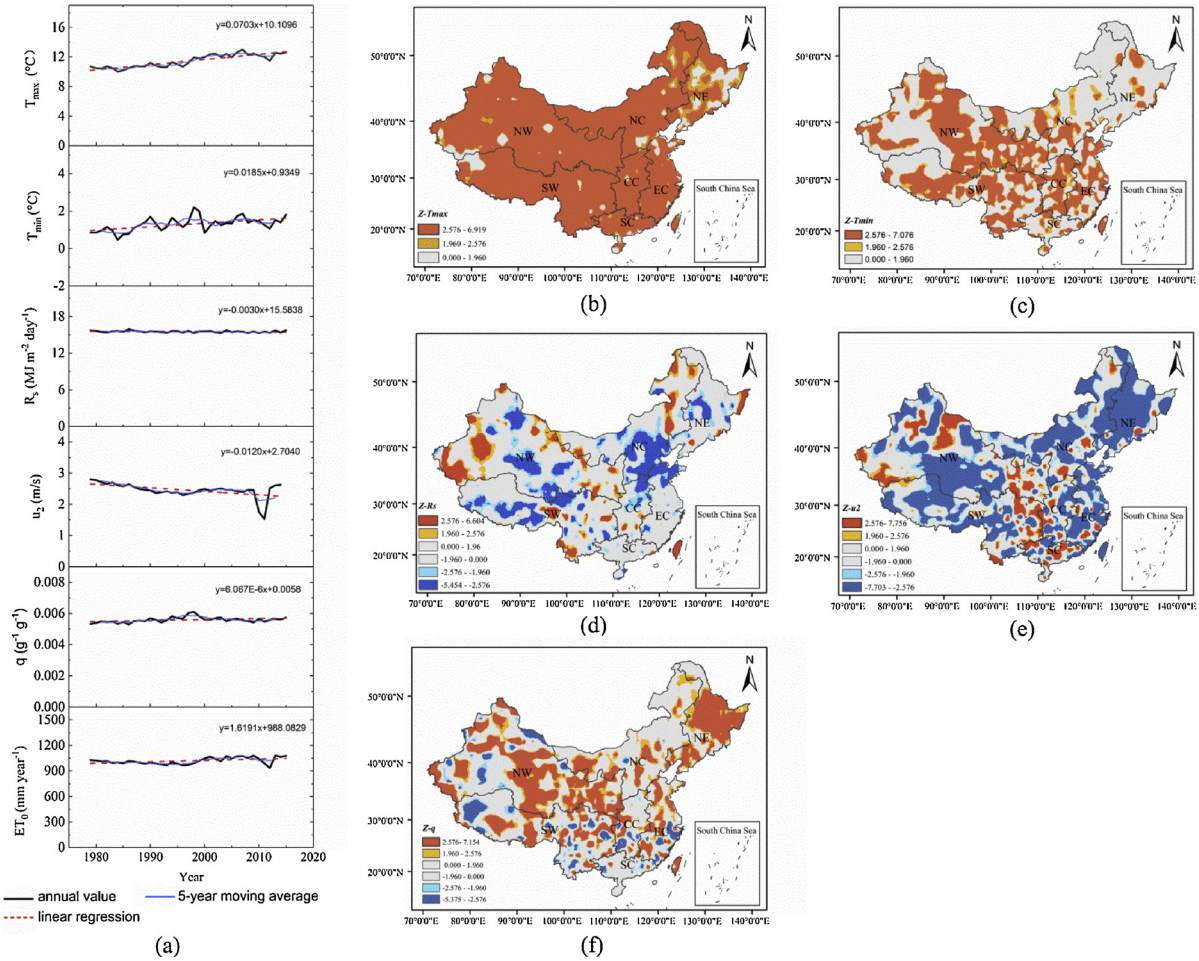

Fig. 2. Spatial and temporal variation of meteorological factors and annual ET_0. (a) reveals the annual value, linear regression and 5-year moving average of five variables and ET_0. (b)-(f) illustrates the statistic Z in M-K test of annual T_{max} (°C), *Tmin* (°C), R_s (W·m^{-2}), u_2 (m·s^{-1}) and, q (kg·kg^{-1}) over China respectively, and the insignificant regions ($|Z| < 1.96$) are in white color.

Table 2
Statistics results for meteorological factors and ET_0 in different regions.

Region	Statistics	Variables				
		T_{max}	T_{min}	R_s	u_2	q	ET_0
NW	Z	4.342**	1.844*	0.105	−1.073	1.707	1.434
	β	0.087	0.026	0.029	−0.006	7e-6	2.684
NC	Z	3.901**	1.102	−0.753	−2.237*	1.214	0.855
	β	0.061	0.014	−0.068	−0.014	5e-6	0.950
NE	Z	2.739**	0.498	−0.635	−3.432**	2.646**	−0.888
	β	0.038	0.004	−0.046	−0.022	1E-5	−0.986
SW	Z	4.548**	1.991*	−0.620	−1.308	0.589	2.200*
	β	0.086	0.024	−0.077	−0.01	4e-6	2.355
CC	Z	4.013**	2.338*	−0.827	−0.877	0.761	1.124
	β	0.049	0.019	−0.108	−0.006	5e-6	1.237
EC	Z	4.079**	2.024*	−1.081	−2.768**	1.107	0.078
	β	0.045	0.017	−0.120	−0.019	7e-6	0.033
SC	Z	3.536**	1.304	−0.256	−0.116	−0.048	1.596
	β	0.036	0.009	−0.029	−0.001	−1e6	1.555

Z: Mann-Kendall test statistic, β: Sen's slope estimator.
* Statistically significant trends at the 5% significance level.
** Statistically significant trends at the 1% significance level.

coefficient of q (Sq) decreased from west to east, which was different from the distribution of the aforementioned meteorological factors. Based on the sensitivity coefficients of meteorological variables in different regions, the driving force of ET_0 is derived. In EC, CC, NE, NC and NW, q plays the predominant role in the sensitivity of ET_0, while ET_0 in SC and SW is most sensitive to *Tmax* and R_s, respectively.

3.4.2. Spatial distribution of contribution rates

The contribution rate of a meteorological factor indicates how the variation of the factor changes ET_0, which is calculated by multiplying the partial derivate by the change rate of a variable. The results of contribution rates in Fig. 8 illustrate that the contribution rate of *Tmax* is positive over most parts of China and decreases progressively from west to east. The negative contribution rate of *Tmin* was more partially distributed in NE, SW and NW. The contribution rate of R_s showed an unremarkable distribution pattern that it was positive in the western and central parts of China, while the negative contribution rate of R_s was found in southwest and eastern China. Most regions in China exhibited a negative contribution rate of wind speed, except the central part of China and some areas in NW, and as for the contribution rate of q, it can be noticed that NE showed a wide-range negative contribution rate of q. On a regional scale, only the ET_0 of NE was dominated by the variation of wind speed, while the predominant contribution rate in other regions of China was by *Tmax*. On a national scale, the highest contribution rate was *Tmax* (0.00757), followed by q (-0.00198), u_2 (-0.00191), *Tmin* (0.00119) and R_s (-0.00017). Comparing the sensitivity coefficients and contribution rates of five variables both regionally and nationally, the more sensitive factor q is incapable of dominating the variation of ET_0 in most regions, while *Tmax* and u_2 play more important roles in changing ET_0 (see Fig. 9).

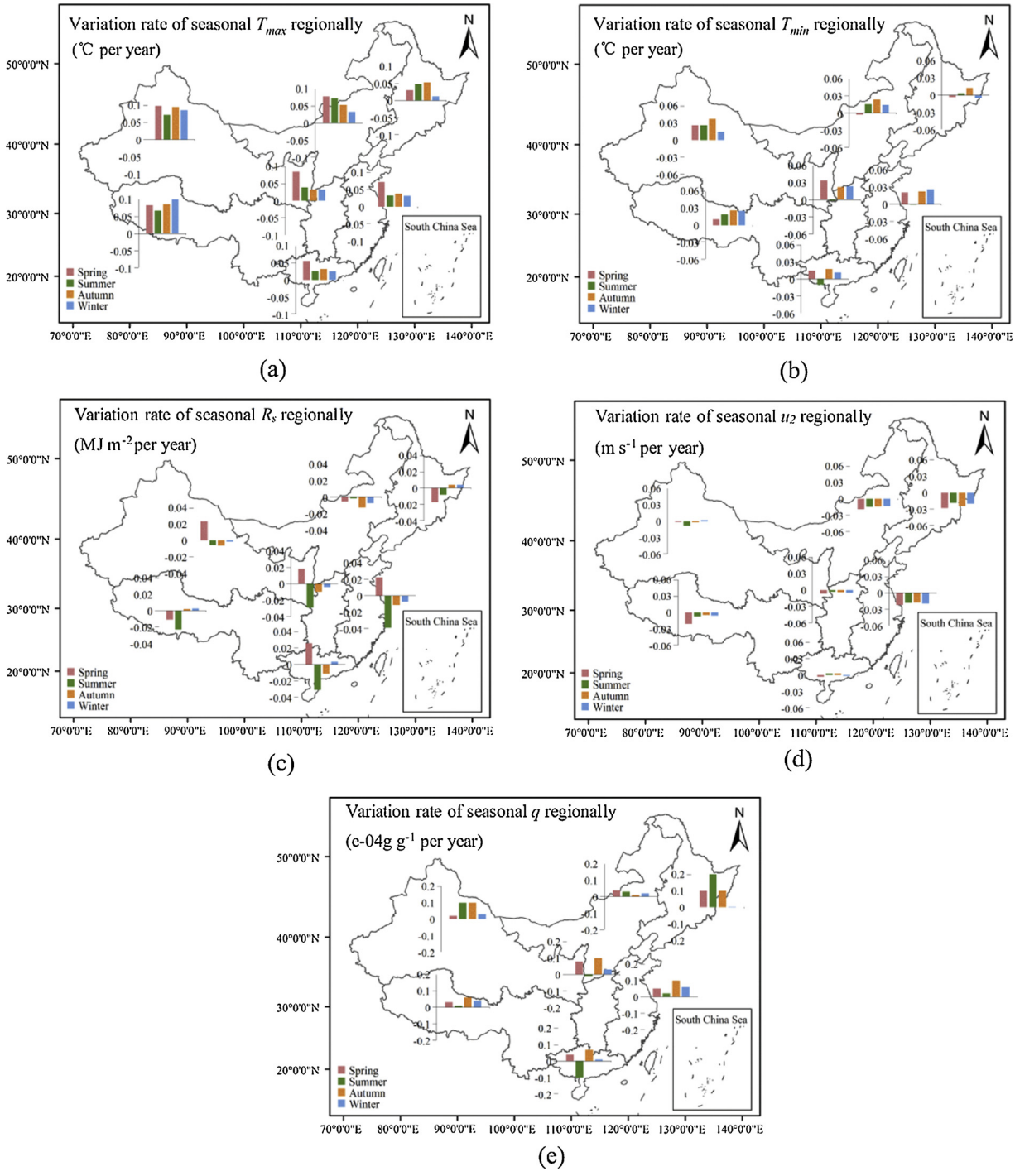

Fig. 3. Regional variation rate of seasonal meteorological variables over China from 1979 to 2015. (a)-(e) illustrate the variation rates of *Tmax*, *Tmin*, R_s, u_2, and q, respectively.

3.5. Trends of aridity index

AI, combined with the variations of ET_0 and precipitation, reveals that a decreasing *AI* may be caused by an increase in precipitation or decrease in ET_0. From the observation of the trend analysis result in Fig. 10a, annual precipitation increases steadily over the study period at a rate of 28 mm per decade, and *AI* decreases at a rate of 0.014 per decade. Before 1996, the increasing precipitation and decreasing ET_0 both resulted in a decrease in *AI*, while after 1996, the driver of the decreasing *AI* was the moderate increase in precipitation. Based on this interannual trend analysis, water availability for rainfed agriculture seems to increase owing to the persistent increase in precipitation, and even the water demand shows an increasing trend in recent years. We also calculate the dispersion degree of interannual ET_0 and precipitation. The remarkable increase in the standard deviation of precipitation (Fig. 10b) illustrates that increased rainfall contrasts both spatially and temporally. The distribution of statistic *Z* of M-K test (Fig. 10c) shows that the significant decreasing *AI* occurs in NW and SW, which is similar to the distribution of Z of precipitation in Fig.10d.

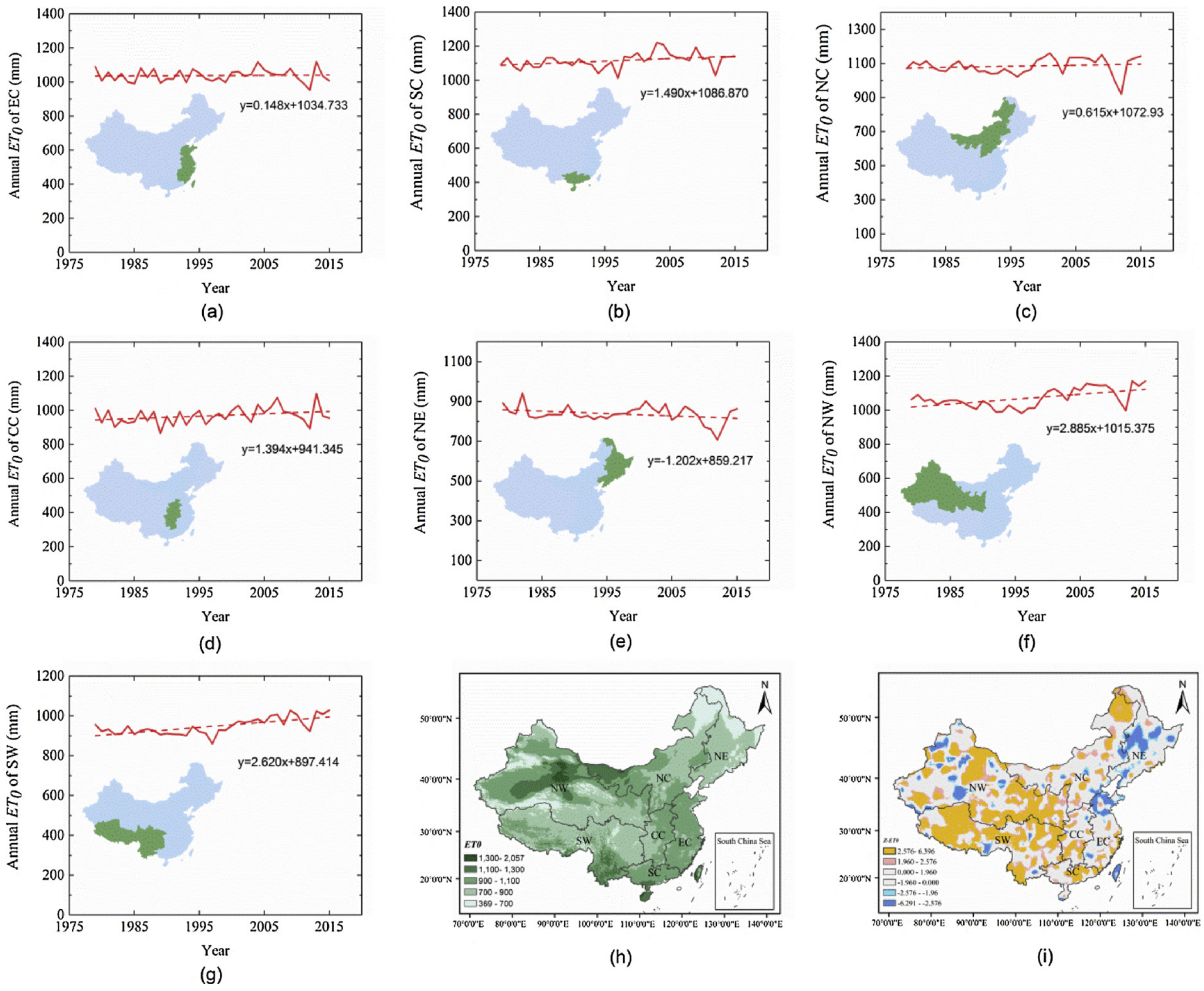

Fig. 4. Variations of annual ET_0 of different regions in China from 1979 to 2015. The rates of linear regression equations in (a)-(g) are 0.148 (EC), 1.490 (SC), 0.615 (NC), 1.394 (CC), -1.202 (NE), 2.885 (NW), and 2.620 mm per year (SW), respectively. (h) and (i) illustrate the average value and MK test statistics of annual ET_0 over China.

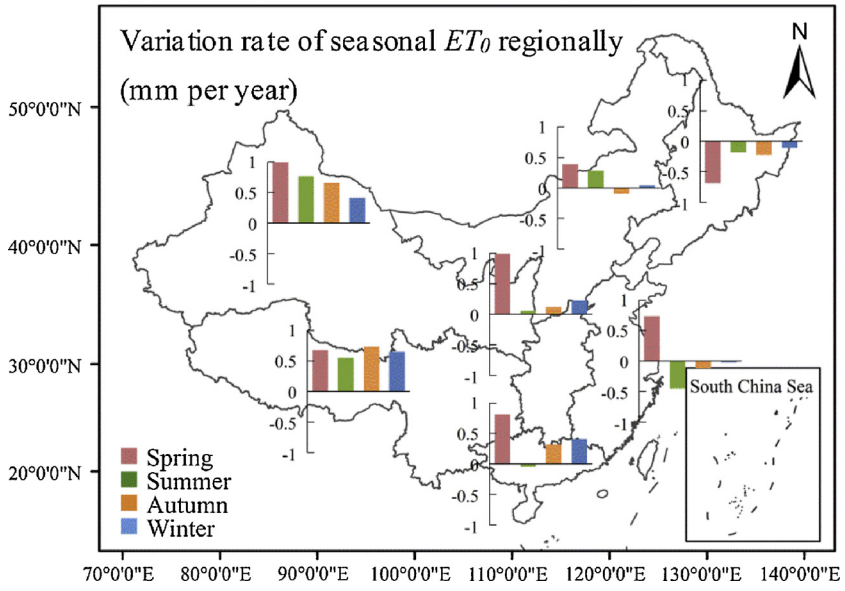

Fig. 5. Seasonal trend of ET_0 over China in.1979–2015.

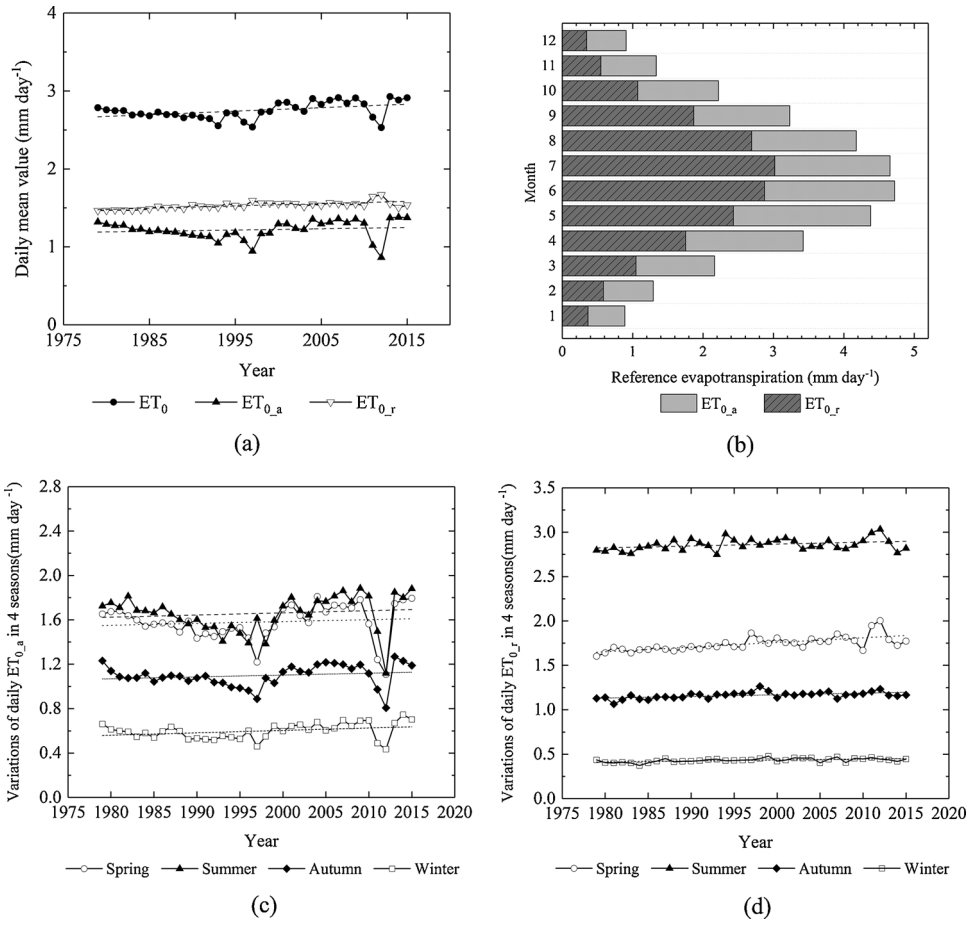

Fig. 6. Variation of ET_{0_a} and ET_{0_r} from 1979 to 2015 over China. (a) and (b) illustrate the interannual trend and annual distribution of ET_{0_a} and ET_{0_r}, (c) and (d) illustrate the interannual trend of seasonal ET_{0_a} and ET_{0_r} respectively.

4. Discussion

4.1. Variation of climate

An unprecedented increasing trend of air temperature over the past thousands of years has indicated that global warming is undisputed. Most parts of China are suffering from warming based on the analysis of CMFD in this study, which is in accordance with most research on variations of air temperature in China over the past few decades (Cui et al., 2017). The predominant reason to explain the wide-range warming is the increase in greenhouse gas emissions caused by population growth and economic development, which also affect radiation to some extent. A relatively moderate decreasing trend of u_2 is found over China during the study period, and the same conclusions can be found in other relevant research (Wang et al., 2012). The distribution of variation in u_2 is irregular in this study, in that a strong decrease occurs in NE, NC and EC, while other regions exhibit smoother decreases in u_2. The 1990s seem to be a time node in which the trends of five meteorological factors started to change, especially q and $Tmax$.

The spatiotemporal dynamics of the five meteorological factors in this study basically conform to many studies on climate change, while there are some delicate differences in spatial distribution, which can be attributed to the form of meteorological data and spatial interpolation. The dataset in this paper is based on grid meteorological data, while most research draws conclusions using meteorological station data.

4.2. The impacts of climate change on the variation of ET_0

It is a common view that the reference evapotranspiration will increase owing to the increases in temperature, radiation, and u_2 and decreasing humidity, while conclusions in many studies from several decades before the 2000s found that ET_0 had decreased along with an increasing temperature. ET_0 over China during 1997–2015 shows an increasing trend accompanied by an increase in air temperature and humidity, as well as a decrease in wind speed, in this study. It exactly illustrates that the variation of ET_0 is affected by many factors and each factor carries a different weight. The obvious valley values of annual ET_0 and ET_{0_a} occurring in 2012. A similar phenomenon can be found in Wang et al. (2017), in that there is an obvious valley value of annual ET_0 occurring in 2012. And these obvious valley values of annual ET_0 and ET_{0_a} in 2012 can be attributed to the low surface air temperature and wind speed. A feasible explanation of low air temperature could be the extreme La Niña event happened in September 2011 which created an extreme cold winter in Asia and Europe in early 2012. The monthly wind speed in 2011, 2012 and 2013 over China were compared and it was found that the abrupt dropping of wind speed mainly occurred in northern China during May-September. A valley value of wind speed in 2012 over northern China also can be found in Lu et al.(2017) while there is few research about the abrupt dropping of wind speed in one year. A feasible explanation of the wind speed anomaly in 2012 could be the significant weak East Asian summer monsoon in 2012 and it needs a further discussion.

Based on the contribution rate of climatic factors, many studies emphasized that the trend of u_2 dominates the variation of evaporative demand by changing the aerodynamic component. It can be seen that the paradox of ET_0, a decreasing ET_0 coupled with increasing air temperature, existed before the 1990s owing to the relatively large decrease in near-surface wind speed. However, after the 1990s, the positive

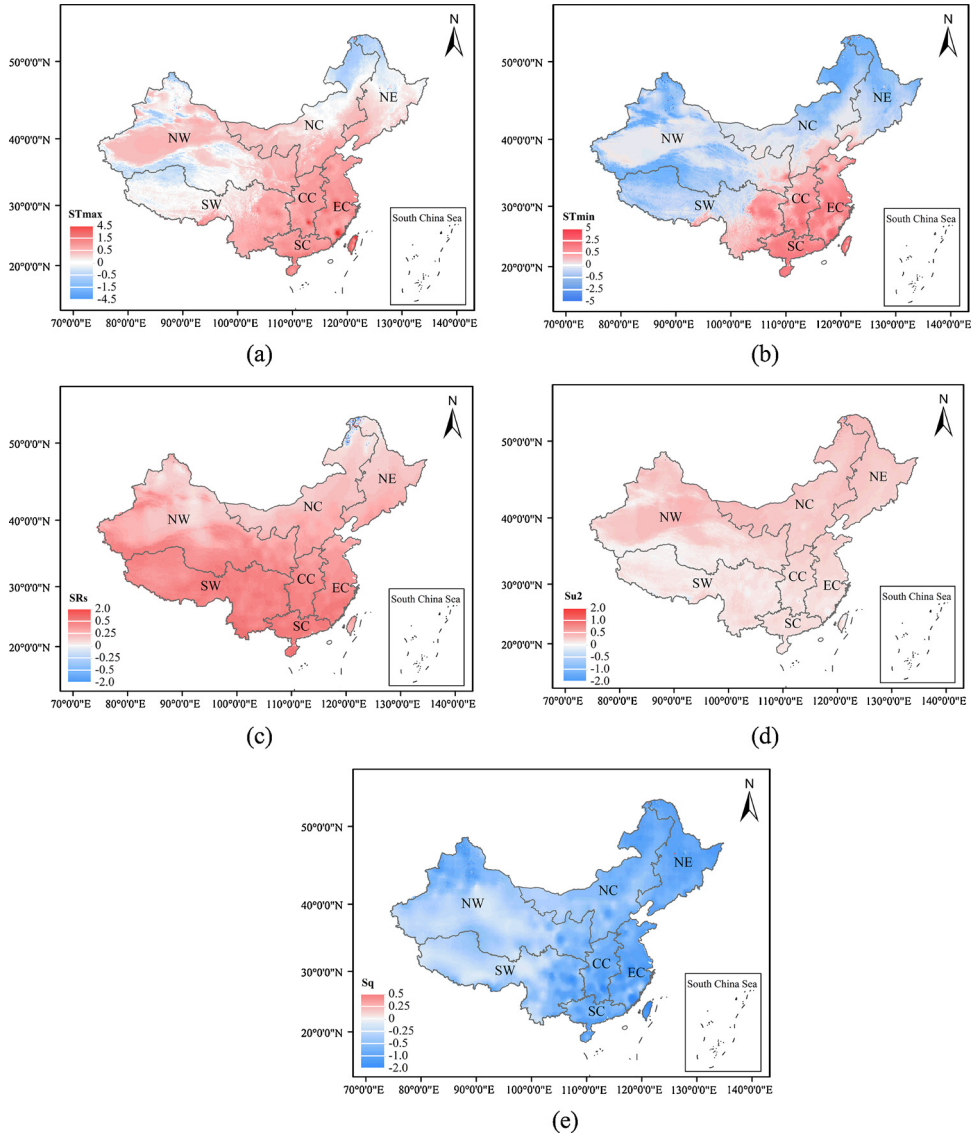

Fig. 7. Annual sensitivity coefficients of meteorological factors on ET_0 over China from 1979 to 2015.

effect on ET_0 by increasing air temperature exceeded the negative effect on ET_0 by decreasing wind speed. The sensitivity analysis in this study illustrates that the ET_0 over China is most sensitive to q (-0.65), followed by *Tmax* (0.38), R_s (0.33), u_2 (0.20) and *Tmin* (0.02), which is consistent with the result of sensitivity analysis in Liu and Zhang (2011). Meanwhile, due to the relatively large increase in *Tmax*, the positive variation of annual ET_0 caused by *Tmax* is larger than other variables and the variation of q is relatively small in that the contribution rate of q is smaller than *Tmax*, even though the sensitive coefficient of q is twice that of *Tmax*. Meanwhile, monthly and seasonal results of ET_{0_r} and ET_{0_a} over China show that ET_0 has a more similar trend of ET_{0_a}, which highlights the importance of the aerodynamic component in affecting ET_0 during spring and summer.

On a regional scale, the highest increase in ET_0 is found in SW, and the other regions show a smoother increase, except that NE has experienced a slight decrease in ET_0 over the study period. Similar spatiotemporal characteristics of ET_0 during the corresponding time series can be found in (Zeng, Song et al., 2010). Thomas (2000) emphasized the wind speed in changing ET_0 in water-limited areas of west China. However, in this study, only the desert regions in NC show a significant decrease in u_2 so that the contribution rate of u_2 is remarkable. The variation of wind speed in NW, another desert region of China, is uneven, as the partial mountainous area there reveals a significant increase, which reduces the absolute value of the u_2 contribution rate. Another region greatly influenced by wind speed is EC, where the impact on ET_0 of *Tmax* is counteracted by the largest decrease in wind speed and radiation to a great extent. The high altitude in SW makes ET_0 sensitive to R_s, while *Tmax* has the largest contribution rate in SW owing to the remarkable increase in *Tmax*.

We also use the contribution analysis method developed by Yin et al. (2010). The result shows an abnormal contribution rate of air temperature in parts of NW, NC and NE, where the air temperature several days a year is close to zero. According to the formulation of the contribution rate, the relative change in a meteorological factor is derived by dividing the annual trend by the annual average value of a factor, and this may result in infinite relative change. Thus, the method developed by Liu et al. (2009) was used to evaluate the contribution rate. Simple rates or coefficients would mask the spatiotemporal features of regional ET_0 and climate. Thus, according to the results of the regional sensitivity and contribution rate analysis, we recommend using another improved geographical division method that can reflect the characteristics of ET_0 and meteorological factors more.

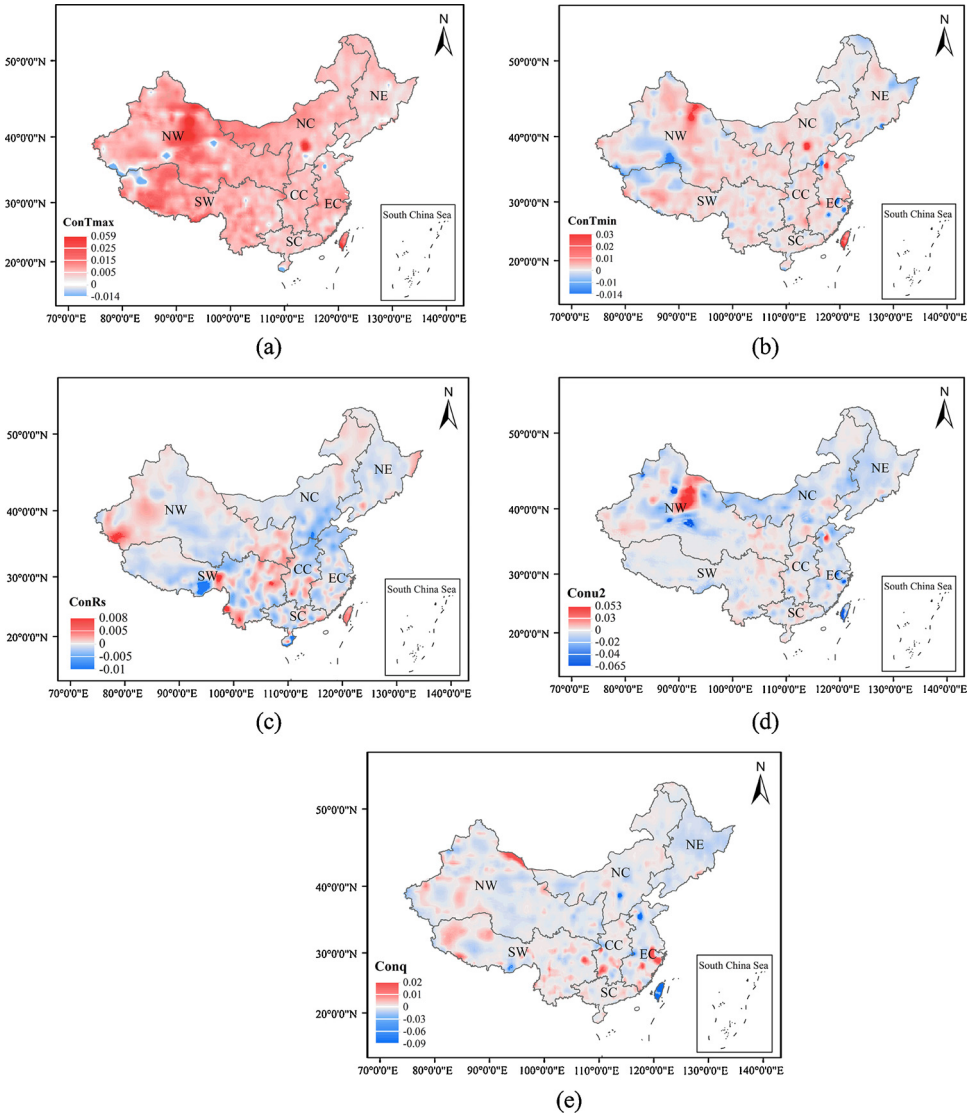

Fig. 8. Contribution rates of five meteorological factors to ET_0 over China from 1979 to 2015.

4.3. Impact of the variation of AI and ET_0 on agricultural water management

The result of the variation of *AI* over China in this study shows a decreasing trend, which means a wetter climate in China. A decreasing pattern of *AI* in different regions of China can also be found in many existing studies (Huo et al., 2013; Wang et al., 2014). The decreasing trend of *AI* in northeastern China in Liu and Zhang (2013) stopped in approximately 1994, and this time point is close to the time in which the valley value of annual ET_0 happens in this study (Fig. 3). In this study, the variation of *AI* is attributed to both the decrease in ET_0 and increasing precipitation before 1996 and depends more on increasing precipitation after 1996. On a regional scale, the significantly decreasing *AI* in NW and SW accompanied by significantly increasing ET_0 and precipitation reveals that the increasing trend of precipitation is more significant than ET_0 in SW and NW.

Some research suggests an adjustment of agricultural water supply due to the variations of ET_0 and *AI* (Estes et al., 2014; Fan et al., 2016). Although annual ET_0 in most of China reveals a significant increasing trend after 1996, the *AI* shows a decreasing trend due to the remarkable increase in precipitation. This trend result suggests an adjustment of agricultural water supply that regulators could reduce the water supply for irrigation with scientific technology because the increase of water availability is more significant than the increase of ET_0. However, this opinion is derived based on the scientific utilization of water resources. Meanwhile, the obviously increasing standard deviation of precipitation means uneven and erratic rainfall within a year, which would increase the vulnerability for agriculture, especially rainfed agriculture. Thus, determining the variations of *ET* and *AI* for specific kinds of crops and types of agriculture is a direction of future research.

5. Conclusions

The previous analysis of climatic factors and ET_0 indicates that there has been a remarkable increase in ET_0 over most parts of China since the 1990s, accompanied by significant increases in air temperature and humidity, as well as decreases in wind speed and radiation. Only northeast China exhibits a decreasing trend of ET_0 that is consistent with the variation of wind speed and is opposite to the trend of humidity. The most obvious increase in ET_0 is found in northwest China, where a prominent increase in air temperature occurs. The variation of ET_0 in eastern China is unremarkable.

The sensitivity analysis quantifies the sensitivities of every meteorological variable to ET_0, indicating that annual ET_0 over China is most sensitive to humidity, followed by air temperature, radiation and wind speed. ET_0 of most areas in China is most sensitive to humidity,

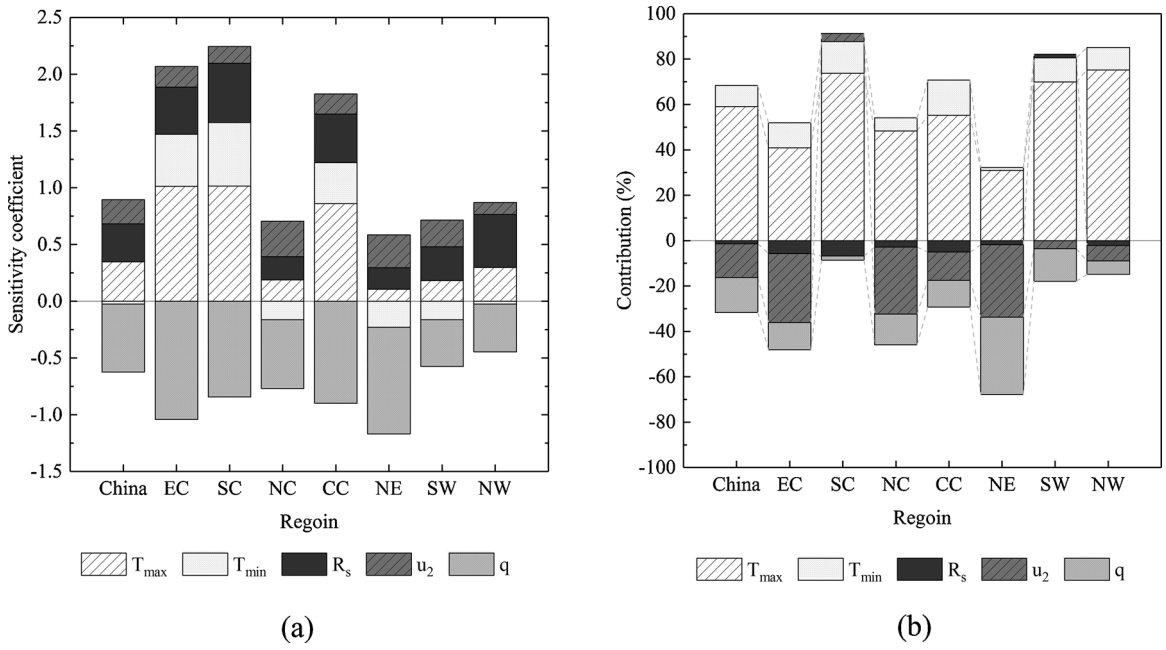

Fig. 9. Sensitivity coefficients and contribution rates of five meteorological factors.

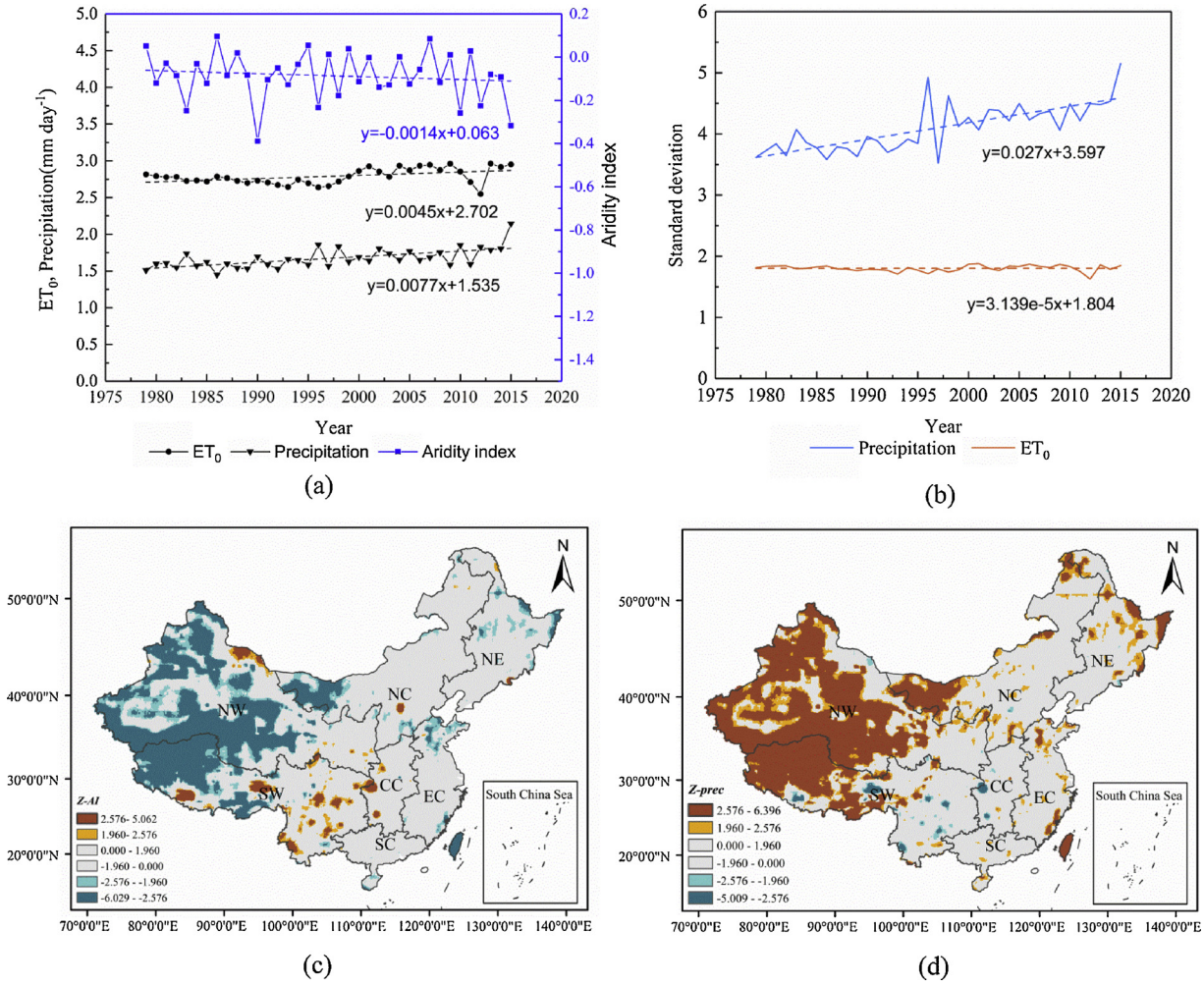

Fig. 10. Comparisons of annual ET_0, precipitation and *AI*. (a) reveals the annual trends of ET_0, precipitation and *AI*, (b) reveals the standard deviations of annual precipitation and ET_0. (c) and (d) illustrates the statistic *Z* of *AI* and precipitation respectively.

while the ET_0 of southwest and southern China is most sensitive to radiation and air temperature, respectively. The variation in humidity more easily changes ET_0 than other climatic factors over China. The sensitivity of a meteorological variable to ET_0 can be related to the variable itself and the magnitudes of other variables; in other words, the same variations of a variable will cause different levels of ET_0 change when other variables have different magnitudes. It can explain the differences in sensitivity of climatic variables in different regions.

The contribution rate of each meteorological variable is also assessed in our study. The result emphasizes the increase in temperature in changing ET_0 over China since the 1990s, especially in northeast China. Due to the variations in variables and the sensitivities of variables to ET_0, the contribution rates vary spatially and temporally. Since the 1990s, the impact of temperature on ET_0 offsets the decrease in ET_0 caused by the gradually decreasing wind speed and increasing humidity in most parts of China. However, the decrease in wind speed and increase in humidity still play dominant roles in the variations of ET_0 in northeast China, which decreases during the study period. The 'evapotranspiration paradox' occurred before the 1990s in China, which should be mainly attributed to the declining wind speed. Therefore, the trend of meteorological factors is essential to analyze the variation of ET_0.

The increasing ET_0 reveals the increasing water demand of crops for evapotranspiration. However, according to the decrease of AI in China, a decrease in unit irrigation water demand can be derived on the premise that utilize water resources properly and adequately. Meanwhile, the more uneven precipitation also raises the importance of adaption strategies for agricultural water management. Thus, under the changing climate, the long-term agricultural water management should be adopted for the continued development.

Funding sources

This work was supported by the National Key Research and Development Program of China [No.2017YFC0403504] and the National Science Foundation of China [No.51479119 and 51579064].

Declarations of interest

None.

References

Allen, R.G., PEREIRA, L.S., RAE, D., SMITH, M., 1998. Crop evapotranspiration-Guidelines for computing crop water requirements. FAO Irrig. Drain. Pap. 56https://doi.org/10.1016/j.eja.2010.12.001. 300, 300.

Chen, S., Liu, Y., Thomas, A., 2006. Climatic change on the Tibetan Plateau: potential evapotranspiration trends from 1961–2000. Clim. Change 76 (3), 291–319. https://doi.org/10.1007/s10584-006-9080-z.

Chen, Y., Yang, K., He, J., Qin, J., Shi, J., Du, J., He, Q., 2011. Improving land surface temperature modeling for dry land of China. J. Geophys. Res. Atmos. 116 (20), 1–15. https://doi.org/10.1029/2011JD015921.

Cui, L., Wang, L., Lai, Z., Tian, Q., Liu, W., Li, J., 2017. Innovative trend analysis of annual and seasonal air temperature and rainfall in the Yangtze River Basin, China during 1960–2015. J. Atmos. Sol. Phys. 164, 48–59. https://doi.org/10.1016/j.jastp.2017.08.001.

Dai, A., 2006. Recent climatology, variability, and trends in global surface humidity. J. Clim. 19. https://doi.org/10.1175/JCLI3816.1.

Darshana, Pandey, A., Pandey, R.P., 2013. Analysing trends in reference evapotranspiration and weather variables in the Tons River Basin in Central India. Stoch. Environ. Res. Risk Assess. 27 (6), 1407–1421. https://doi.org/10.1007/s00477-012-0677-7.

Estes, L.D., Chaney, N.W., Herrera-Estrada, J., Sheffield, J., Caylor, K.K., Wood, E.F., 2014. Changing water availability during the African maize-growing season. Environ. Res. Lett. 9 (7), 1979–2010. https://doi.org/10.1088/1748-9326/9/7/075005.

Fan, Z., Thomas, A., 2018. Decadal changes of reference crop evapotranspiration attribution: spatial and temporal variability over China 1960–2011. J. Hydrol. (Amst.) 560, 461–470. https://doi.org/10.1016/j.jhydrol.2018.02.080.

Fan, J., Wu, L., Zhang, F., Xiang, Y., Zheng, J., 2016. Climate change effects on reference crop evapotranspiration across different climatic zones of China during 1956–2015. J. Hydrol. (Amst.) 542, 923–937. https://doi.org/10.1016/j.jhydrol.2016.09.060.

Feng, J., Yan, D., Li, C., Yu, F., Zhang, C., 2014. Assessing the impact of climatic factors on potential evapotranspiration in droughts in North China. Quat. Int. 336, 6–12. https://doi.org/10.1016/j.quaint.2013.06.011.

Gocic, M., Trajkovic, S., 2013. Analysis of changes in meteorological variables using Mann-Kendall and Sen's slope estimator statistical tests in Serbia. Glob. Planet. Change 100, 172–182. https://doi.org/10.1016/j.gloplacha.2012.10.014.

Gong, L., Xu, C., Chen, D., Halldin, S., Chen, Y.D., 2006. Sensitivity of the Penman–Monteith reference evapotranspiration to key climatic variables in the Changjiang (Yangtze River) basin. J. Hydrol. (Amst.) 329 (3), 620–629. https://doi.org/10.1016/j.jhydrol.2006.03.027.

Hirsch, R., Slack, J.R., 1984. Non-parametric trend test for seasonal data with serial dependence. Water Resour. Res. 20. https://doi.org/10.1029/WR020i006p00727.

Hoffman, F.M., 2010. Recent Decline in the Global Land Evapotranspiration Trend Due to Limited Moisture Supply Introduction More Than Half of the Solar Energy Absorbed by Land Surfaces.

Huo, Z., Dai, X., Feng, S., Kang, S., Huang, G., 2013. Effect of climate change on reference evapotranspiration and aridity index in arid region of China. J. Hydrol. (Amst.) 492. https://doi.org/10.1016/j.jhydrol.2013.04.011.

Liu, X.M., Zheng, H.X., Liu, C.M., 2009. Sensitivity of the potential evapotranspiration to key climatic variables in the Haihe River Basin. J. Nat. Resour. Life Sci. Educ. 31.

Liu, X., Luo, Y., Zhang, D., Zhang, M., Liu, C., 2011. Recent changes in pan-evaporation dynamics in China. Geophys. Res. Lett. 38 (13), 10–13. https://doi.org/10.1029/2011GL047929.

Liu, S.M., Xu, Z.W., Zhu, Z.L., Jia, Z.Z., Zhu, M.J., 2013. Measurements of evapotranspiration from eddy-covariance systems and large aperture scintillometers in the Hai River Basin, China. J. Hydrol. 487, 24–38. https://doi.org/10.1016/j.jhydrol.2013.02.025.

Liu, C., Zhang, D., 2011. Temporal and spatial change analysis of the sensitivity of potential evapotranspiration to meteorological influencing factors in China. Acta Geographica Sinica 66.

Liu, X., Zhang, D., 2013. Trend analysis of reference evapotranspiration in Northwest China: the roles of changing wind speed and surface air temperature. Hydrol. Process. 27. https://doi.org/10.1002/hyp.9527.

Lu, J., Yan, J., Wang, P., Liu, Y., 2017. Wind speed change characteristics of Shaanxi-Gansu-Ningxia Area in 1960-2014. J. Desert Res. 37 (3), 554–561. https://doi.org/10.7522/j.issn.1000-694X.2016.00114.

Luxmoore, R.J., Stolzy, J.L., Holdeman, J.T., 1981. Sensitivity of a soil-plant-atmosphere model to changes in air temperature, dew point temperature, and solar radiation. Agric. Meteorol. 23, 115–129. https://doi.org/10.1016/0002-1571(81)90094-7.

McCuen, R.H., 1974. A sensitivity and error analysis Cf procedures used for estimating evaporation. JAWRA J. Am. Water Resour. Assoc. 10 (3), 486–497. https://doi.org/10.1111/j.1752-1688.1974.tb00590.x.

Mcmahon, T., Peel, M., Lowe, L., Srikanthan, R., Mcvicar, T., 2012. Estimating actual, potential, reference crop and pan evaporation using standard meteorological data: a pragmatic synthesis. Hydrol. Earth Syst. Sci. Discuss. 9. https://doi.org/10.5194/hessd-9-11829-2012.

McVicar, T.R., Van Niel, T.G., Li, L., Hutchinson, M.F., Mu, X., Liu, Z., 2007. Spatially distributing monthly reference evapotranspiration and pan evaporation considering topographic influences. J. Hydrol. (Amst.) 338 (3), 196–220. https://doi.org/10.1016/j.jhydrol.2007.02.018.

McVicar, T.R., Roderick, M.L., Donohue, R.J., Li, L.T., Van Niel, T.G., Thomas, A., Dinpashoh, Y., 2012. Global review and synthesis of trends in observed terrestrial near-surface wind speeds: implications for evaporation. J. Hydrol. (Amst.) 416–417, 182–205. https://doi.org/10.1016/j.jhydrol.2011.10.024.

Odhiambo, L., Wright, W., Yoder, R., 2005. Evaluation of methods for estimating daily reference crop evapotranspiration at a site in the humid southeast United States. Appl. Eng. Agric. 21. https://doi.org/10.13031/2013.18153.

Partal, T., Kahya, E., 2006. Trend analysis in Turkish precipitation data. Hydrol. Process. 20, 2011–2026. https://doi.org/10.1002/hyp.5993.

Sen, P.K., 1968. Estimates of the regression coefficient based on Kendall's tau. J. Am. Stat. Assoc. 63, 1379–1389. https://doi.org/10.1080/01621459.1968.10480934.

Seo, K.W., Waliser, D.E., Tian, B., Kim, B.M., Park, S.C., Cocke, S., Sohn, B.J., Ishii, M., 2012. Evidence of the recent decade change in global fresh water discharge and evapotranspiration revealed by reanalysis and satellite observations. Asia Pac. J. Atmos. Sci. 48, 153–158. https://doi.org/10.1007/s13143-012-0015-5.

Shen, H., Yapa, P., 1986. Flow resistance of river ice cover. J. Hydraul. Eng. 112. https://doi.org/10.1061/(ASCE)0733-9429(1986)112:2(142).

Stocker, T.F., Qin, D., Plattner, G.-K., Tignor, M., Allen, S.K., Boschung, J., Midgley, P.M., 2014. IPCC, 2013: Climate Change 2013: The Physical Science Basis. Contribution of Working Group I to the Fifth Assessment Report of the Intergovern- Mental Panel on Climate Change. Cambridge University Press.

Tabari, H., Aghajanloo, M.-B., 2013. Temporal pattern of aridity index in Iran with considering precipitation and evapotranspiration trends. Int. J. Climatol. 33. https://doi.org/10.1002/joc.3432.

Tang, W.J., Yang, K., Qin, J., Cheng, C.C.K., He, J., 2011. Solar radiation trend across China in recent decades: a revisit with quality-controlled data. Atmos. Chem. Phys. 11 (1), 393–406. https://doi.org/10.5194/acp-11-393-2011.

Thomas, A., 2000. Spatial and temporal characteristics of potential ET trends over China. Int. J. Climatol. 20. https://doi.org/10.1002/(SICI)1097-0088(20000330)20:4<381::AID-JOC477>3.0.CO;2-K.

Verburg, P., Hecky, R.E., 2003. Wind patterns, evaporation, and related physical variables in Lake Tanganyika, East Africa. J. Great Lakes Res. 29, 48–61. https://doi.org/10.1016/S0380-1330(03)70538-3.

Wang, K., Dickinson, R., Wild, M., Liang, S., 2012. Atmospheric impacts on climatic variability of surface incident solar radiation. Atmos. Chem. Phys. 12. https://doi.org/10.5194/acp-12-9581-2012.

Wang, L., Cao, L., Deng, X., Jia, P., Zhang, W., Xu, X., Chen, Y., 2014. Changes in aridity

index and reference evapotranspiration over the central and eastern Tibetan Plateau in China during 1960–2012. Quat. Int. 349, 280–286. https://doi.org/10.1016/j.quaint.2014.07.030.

Wang, Z., Xie, P., Lai, C., Chen, X., Wu, X., Zeng, Z., Li, J., 2017. Spatiotemporal variability of reference evapotranspiration and contributing climatic factors in China during 1961–2013. J. Hydrol. (Amst.) 544, 97–108. https://doi.org/10.1016/j.jhydrol.2016.11.021.

Xu, J., Peng, S.-Z., Ding, J.-L., Wei, Z., 2010. Evaluation of methods for estimating daily reference crop evapotranspiration based on lysimeter grass experiments. J. Hydraul. Eng. 41.

Xue, B.L., Wang, L., Yang, K., Tian, L., Qin, J., Chen, Y., Li, X., 2013. Modeling the land surface water and energy cycles of a mesoscale watershed in the central Tibetan Plateau during summer with a distributed hydrological model. J. Geophys. Res. Atmos. 118 (16), 8857–8868. https://doi.org/10.1002/jgrd.50696.

Yin, Y., Wu, S., Chen, G., Dai, E., 2010. Attribution analyses of potential evapotranspiration changes in China since the 1960s. Theor. Appl. Climatol. 101 (1), 19–28. https://doi.org/10.1007/s00704-009-0197-7.

Young, I., Zieger, S., Babanin, A., 2011. Global trends in wind speed and wave height. Science (New York, N.Y.) 332. https://doi.org/10.1126/science.1197219.

Zeng, L.-H., Song, K.-S., Zhang, B., Wang, Z.-M., Du, J. 2010. Spatiotemporal variability of reference evapotranspiration over the Northeast region of China in the last 60 Years (Vol. 21).

Zhang, K., Pan, S., Zhang, W., Xu, Y., Cao, L., Hao, Y., Wang, Y., 2015. Influence of climate change on reference evapotranspiration and aridity index and their temporal-spatial variations in the Yellow River Basin, China, from 1961 to 2012. Quat. Int. 380–381, 75–82. https://doi.org/10.1016/j.quaint.2014.12.037.

Zongxing, L., Qi, F., Wei, L., Tingting, W., Yan, G., Yamin, W., Li, L., 2014. Spatial and temporal trend of potential evapotranspiration and related driving forces in Southwestern China, during 1961–2009. Quat. Int. 336, 127–144. https://doi.org/10.1016/j.quaint.2013.12.045.